

## TECHNIQUES FOR NDE OF CLOSED CRACKS

M. Saka<sup>1</sup>, H. Tohmyoh<sup>1</sup>, and Y. Kondo<sup>1</sup>

<sup>1</sup> Department of Mechanical Engineering, Tohoku University, Sendai 980-8579, Japan

**Abstract:** Usually ultrasonic techniques tend to evaluate the closed cracks as smaller than the actual size. In this paper, we describe two strategic techniques for accurately evaluating the closed cracks by means of ultrasound. First, we show the advanced technique utilizing the thermal stress induced by cooling a cracked part. It is shown that a small amount of temperature decrease is effective to open a closed crack and hence to increase the ultrasonic response of the closed crack. Another advanced technique gives the success in quantitative evaluation of both the crack depth and the crack closure stress by nondestructive way. The technique is based on the analysis of inverse problem, and capable of evaluating tightly closed cracks as well as open cracks under a no load condition.

**Introduction:** Ultrasonic techniques have traditionally been used for nondestructive inspection of cracks [1-10]. Usually, nondestructive inspection is carried out when structural components are not in operation. This means that cracks are required to be detected and evaluated under a no load condition. Fatigue cracks are known to close under a no load condition due to plastic deformation in the wake of the crack which is surrounded by an elastic region, and stress corrosion cracking shows closure due to oxide between the mating crack surfaces. Therefore, the no load condition causes a significant problem of crack closure, especially in the ultrasonic techniques. If the closed crack undergoes nondestructive inspection without opening it, the crack will be erroneously evaluated as being smaller than the actual size [11,12]. Recently, the technique called thermosonics combining the sound pulse as the energy source with an infrared camera for monitoring the subsequent photons emitted in the vicinity of a surface or subsurface defect has received considerable attention [13]. The technique is effective for detecting and sizing surface or subsurface closed cracks.

In this paper, we describe some strategic techniques for nondestructive evaluation (NDE) of closed cracks hidden in the components. One advanced technique is an application of cooling to a cracked part for NDE of cracks. Another advanced technique realizes the simultaneous evaluation of both the crack size and the closure stress under a no load condition.

**Difficulties of Sizing Closed Cracks:** Common ultrasonic techniques for the evaluation of crack depth used the reflected and tip-diffracted waves of bulk shear and longitudinal waves and also the surface Rayleigh wave [1-10]. But sizing a tightly closed crack is difficult. The difficulties of sizing closed cracks are due to 1) Reduction in signal intensity caused by the sound transmission through the closed crack surfaces, and 2) Noises from the closed crack surfaces because of the contacting asperities. Figure 1 shows the echo patterns obtained by the tip-diffracted wave method [(a)] and Rayleigh wave method [(b) and (c)] [11]. A fatigue crack in austenitic stainless steel (AISI304) specimen having a size of  $468 \times 38 \times 76$  mm was examined. It is difficult to find the crack-tip signal in Fig. 1(a) obtained by the tip-diffracted wave method (6 MHz,  $45^\circ$  shear wave) under a no loading. The intensity of the tip-diffracted wave is weak, and in the case of closed cracks, it is further weakened by sound transmission through the closed crack surfaces. Because of the low amplitude of the diffracted wave from closed cracks and the high noise-background, signal diffracted from the tip of the crack may approach to the noise level and become undetectable. Hence it is extremely difficult to clearly distinguish the crack-tip signal from back-scattering noises. Also, when the Rayleigh wave method (5 MHz) was used under a no loading, the noises arising from tightly contacting asperities on the crack surfaces made it difficult to detect the crack-tip signal [Fig. 1(b)]. If we open the crack by an additional loading, the echo pattern clearly shows the crack-tip signal [Fig. 1(c)], and we can evaluate the crack depth from the time-of-flight of the crack-tip signal.

**Advanced NDE of Closed Cracks Utilizing Thermal Stress:** In this paper, we propose a strategic technique using thermal stress for NDE of closed cracks. In the previous section, it was shown that additional loading is effective for opening the closed cracks and the ultrasonic response from the crack is enhanced by the loading. The technique proposed here uses the thermal stress induced simply by cooling a cracked part for effectively opening the closed crack. The technique is applicable to the hidden cracks in the components.

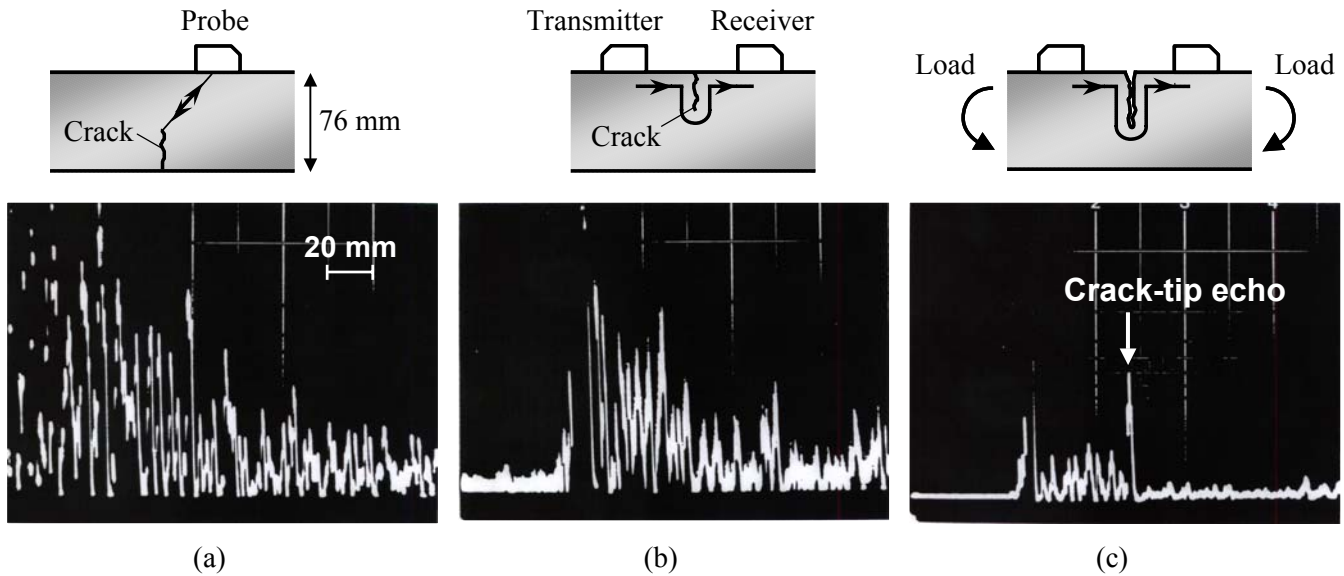


Figure 1 Echo patterns obtained by (a) the tip-diffracted wave method and (b), (c) Rayleigh wave method. Patterns (a) and (b) are obtained under no loading condition and (c) loading condition.

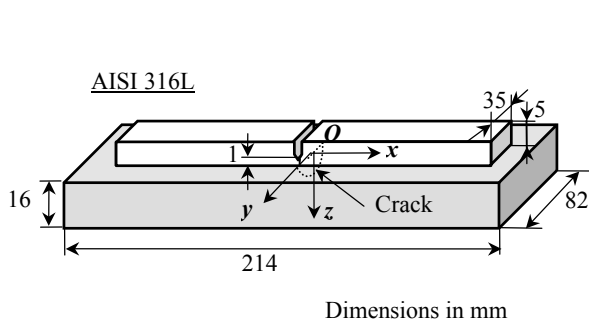


Figure 2 Geometry of specimen to introduce a 3-D fatigue crack.

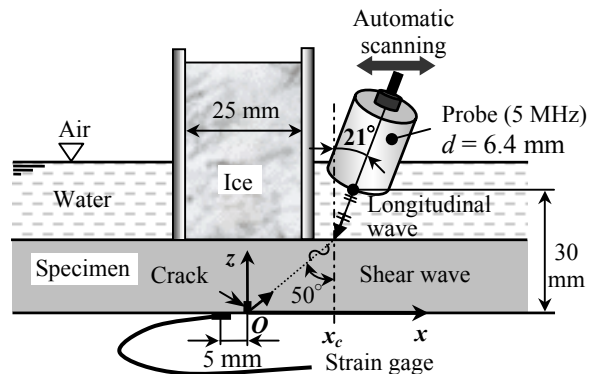


Figure 3 Schematic of ultrasonic testing configuration.

**Experiments:** Let us demonstrate the technique by showing an example. A three-dimensional fatigue crack was introduced in a specimen. The specimen was machined from austenitic stainless steel, AISI316L, of which initial shape is shown in Fig. 2. The dimensions of the bed-plate were  $214 \times 82 \times 16$  mm, on which a narrow strip having the dimensions of  $174 \times 35 \times 5$  mm was remained. A Cartesian coordinates system ( $x, y, z$ ) was chosen such that the origin  $O$  was located at the center of the specimen width on the surface of the bed-plate. An initial notch was introduced in the strip and the fatigue crack was grown from the tip of the initial notch by cyclically loading the plate in four-point bending on the dynamic testing machine. The stress ratio [= minimum load / maximum load] of 0.5 was maintained during the crack growth. The maximum load was 76.4 kN, and the test frequency was 6 Hz. After introducing the fatigue crack, the specimen was machined and polished in  $164 \times 82 \times 15$  mm to remove the narrow strip, leaving a true three-dimensional fatigue crack in the remaining bed-plate.

The ultrasonic testing configuration is illustrated in Fig. 3. The crack was located at the back wall of the specimen. All measurements were performed under the water immersion at room temperature of  $22^\circ\text{C}$ . The ultrasonic probe having the nominal frequency of 5 MHz and the diameter of the piezoelectric element,  $d$ , of 6.4 mm was attached on a  $xyz$ -scanner for automatic scanning. The distance between the probe and the back wall of a

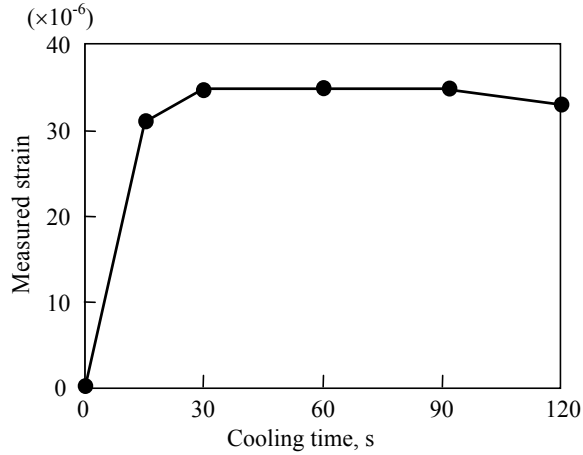


Figure 4 Measured strain plotted as a function of cooling time.

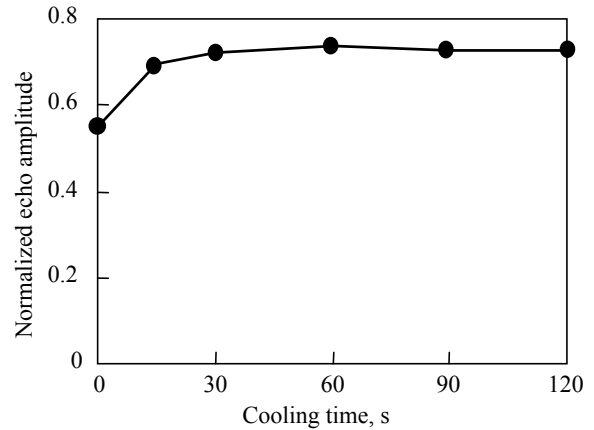


Figure 5 Normalized echo amplitude as a function of cooling time.

specimen was kept at 30 mm. The angle beam technique was adopted in the present study. The incident angle of the longitudinal wave in water was  $21^\circ$ , and its corresponding refracted angle of the shear wave in steel was  $50^\circ$  [14]. The distance  $x_c$  indicates the position on the top surface of the specimen from which the probe can detect the crack by receiving an echo from the corner between the crack and the back wall. A part of the top surface of the specimen was cooled by using the circular cylinder of ice with the diameter of 25 mm, see Fig. 3. The strain gage was glued at 5 mm away from the crack for measuring the strain generated by cooling the cracked part. The ultrasonic response and the strain during the cooling were simultaneously recorded for 120 s after the cooling was started.

Figures 4 and 5 show the measured strain and the ultrasonic echo amplitude as a function of the cooling time, respectively. The ultrasonic echo amplitude in Fig. 5 is normalized with the back-wall echo obtained under the normal incidence at a position where no crack is present, of which value was 7.57 Volts. From Fig. 4, it can be seen that the strain at the back wall surface increases with increasing the cooling time and it saturates after the cooling time of about 30 s. Also the normalized echo amplitude increases with increasing the cooling time and it reaches the maximum value at about 30 s cooling, similarly to the behavior of the strain. The fact shown in Fig. 5 suggested that the effective tensile stress for opening the closed crack was generated by cooling a cracked part and it reduced the influence of the initial closure stress on ultrasonic testing. In the present simple experiment, the ultrasonic echo amplitude was enhanced about 1.3 times as large as that obtained under the no-cooling condition by the induced tensile thermal stress.

**Thermal Stress Analysis:** In the previous section, it was shown that the thermal stress caused by the temperature distribution in the plate specimen effectively opens the closed crack and it enhances the ultrasonic response of the crack.

Figure 6 illustrates a schematic of the stress state of a closed crack just opened. The stress state of Fig. 6(a), at which a crack is just opened by cooling a cracked part, is considered as the superposition of the initial closure stress met by the closed crack [Fig. 6(b)] and the thermal stress working at the position of virtual crack corresponding to the crack position [Fig. 6(c)]. The effect of cooling a cracked part on weakening crack closure stress is schematically illustrated in Fig. 7. The thermal stress increases with increasing the cooling time, and it releases the initial closure stress. If an enough amount of thermal stress for opening the closed crack is generated by cooling the cracked part, the closed crack will fully be opened.

Let us demonstrate the thermal stress caused by cooling a cracked part in some examples of the actual pipe. The tensile thermal stress in the longitudinal direction of the pipe, which is induced by a unit amount of temperature decrease, was calculated by the finite element method. Here, the thermal stress is associated with the

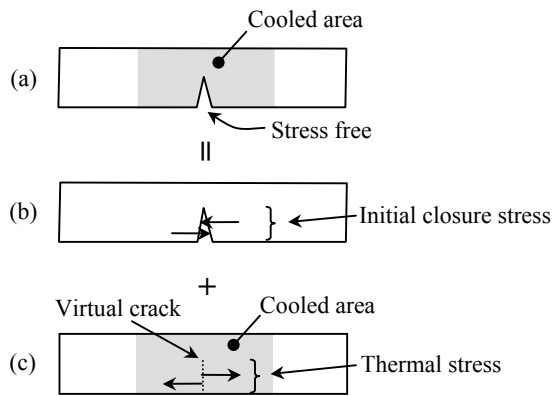


Figure 6 Stress state (a), at which a crack is just opened by cooling a cracked part, expressed by superposing subproblems (b) and (c).

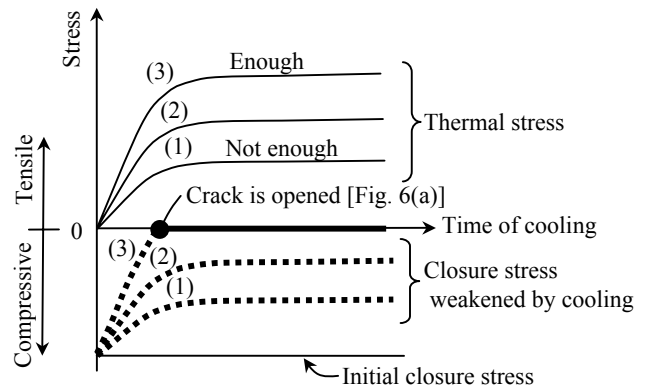


Figure 7 Schematic illustration of the effect of cooling a cracked part on weakening crack closure stress.

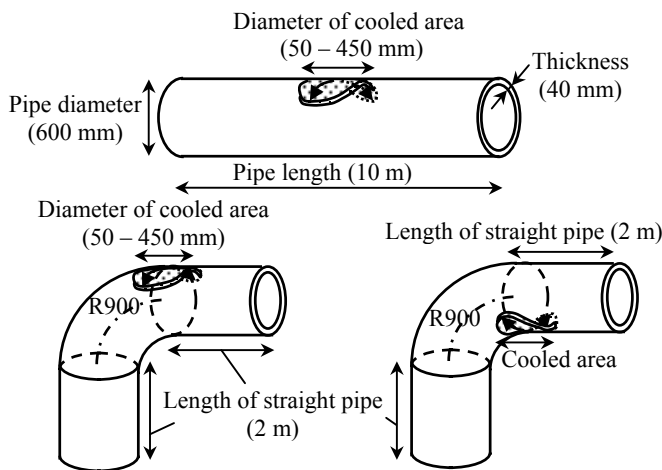


Figure 8 Schematics of straight and bend pipes.

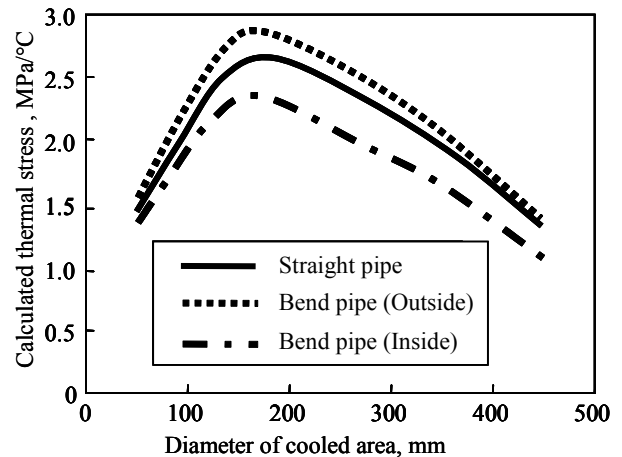


Figure 9 Calculated thermal stress in straight and bend pipes.

stress state shown in Fig. 6(c). The schematics of two pipes having the diameter of 600 mm and the thickness of 40 mm and the cooled areas are shown in Fig. 8. One was straight pipe having the length of 10 m, and another was bend pipe having the curvature of  $1 / 900 \text{ mm}^{-1}$ . The length of the straight parts of the bend pipe was 2 m. The temperature of the cooled area was assumed to be constant for simplicity. By considering the symmetry of the pipes, half parts of the pipes were modeled in the numerical analysis. We assumed the pipes made of AISI316L, and the used data were Young's modulus of 193 GPa, Poisson's ratio of 0.3 and linear expansion coefficient of  $1.6 \times 10^{-5} \text{ 1/}^\circ\text{C}$ . The analysis was carried out for various values of the diameter of cooled area in the range of 50 to 450 mm. The thermal stress in bend pipe was obtained at the outside and inside of the bending part by taking account of its welding location.

Figure 9 shows the calculated thermal stress generated on the inner walls of the pipes in the relation with the diameter of cooled area. The values of the thermal stress at the outside of bend pipe are higher than those of the inside of bend pipe and the straight pipe. For all cooling conditions examined, the values of the maximum thermal stress were generated with the cooled area in the size of around 150 mm diameter, and the values varied from 2.5 to 3.0 MPa/°C. This fact indicates that the temperature decrease of 22 °C, for example, generates the tensile thermal

stress of 55 to 66 MPa in the pipes. By controlling the thermal stress to be so small that no further crack growth occurs, a circumferential closed crack on the inner wall is opened to increase the ultrasonic response.

**Advanced NDE of Closed Cracks Based on Inverse Analysis:** To nondestructively evaluate the closed cracks, Saka and Abé [12], and Saka and Uchikawa [15] have proposed a model of crack closure for the evaluation of closed cracks by using a normally incident longitudinal wave beam. In an attempt to deal with smaller closed cracks an angle beam evaluation approach was developed by Ahmed and Saka [16], and thereafter the method was extended to a number of cases of practical importance [17]. In their methods, however, the closure stress was determined as qualitative representation. To quantitatively evaluate the closure stress of closed cracks together with the crack depth, we show the treatment of ultrasonic NDE of closed cracks as an inverse problem.

**Analysis of Echo Amplitudes:** The tight contact of the two rough crack surfaces leads to transmission, reflection and mode conversion of the reflected wave. If we utilize the large angle of incidence, the back-wall echo does not return back to the ultrasonic probe and eventually the peak-to-peak amplitude of the received signal for the case of a closed crack,  $p$ , can be expressed by the following equation [18]:

$$p = \mathcal{P} p_c, \quad (1)$$

where  $p_c$  is the peak-to-peak amplitude of the received signal due to the reflection experienced at the open crack surface. The quantities  $p$  and  $p_c$  are experimentally measurable, thereby leaving the reflection coefficient  $\gamma$  as a determinable quantity. In the modeling of crack closure, these  $p_c$  and  $\gamma$  are expressed in terms of crack depth and crack closure stress, respectively.

Ultrasonic response of a closed crack, which was introduced in an AISI304 specimen with the thickness of 12 mm, obtained under the state of different applied loading is presented as a function of normalized probe position,  $\bar{x} = (x - x_c)/d$ , in Fig. 10. The amplitude of the first back wall echo of the incidence wave,  $p$ , was normalized by

$$p^{ex} = p/p_0^n, \quad (2)$$

where  $p_0^n$  is the amplitude of the reference echo obtained under the normal incidence at a position where no crack is present. From the figure it is clear that the ultrasonic response decreases with the increase in the absolute value of the applied stress,  $\sigma_{pa}$ . For an additional stress of  $-71$  MPa, the maximum echo amplitude is reduced by 66 % of that of the open condition. Ultrasonic response of a closed crack is highly sensitive to its closure stress. Coefficient  $\gamma$  is determined by the ratio of echo amplitude of closed crack to that of open crack for each measurement position in the range of  $-0.7 \leq \bar{x} \leq 0.7$ . In some specimens, the ultrasonic response was measured under additional compressive stress by applying compression, and  $\gamma$  is determined for each stress condition.

**Calibration Equations:** At no load condition, a crack suffers the initial closure stress. The initial closure stress  $\sigma_{pi}$  of crack was determined by standard compliance technique [19,20]. The crack closure stress at additional load condition is determined as  $\sigma_p = \sigma_{pa} + \sigma_{pi}$ . For the closed crack having initial closure stress of  $-58.8$  MPa, the values of  $\gamma$  are calculated from the response measured under different applied stresses. The results for probe position  $\bar{x} = 0.0$  are plotted in Fig. 11 against the closure stress. From the plot, it is clear that the reflection coefficient decreases with the increase in absolute value of closure stress. The  $\gamma$  curves for different cracks were observed to lie together along the dotted curve shown in the figure, and we find  $\gamma$  is independent of the crack depth. From this plot the variation of  $\gamma$  as a function of  $\sigma_p$  has been estimated as

$$\gamma = f_1(\bar{\sigma}, \bar{x}), \quad (3)$$

where  $\bar{\sigma} = (\sigma_p - 70)/250$ . The normalized response of the open crack,  $p_c^{es}$ , as a function of normalized crack size,  $\bar{a} (= a/d)$ , has been estimated as

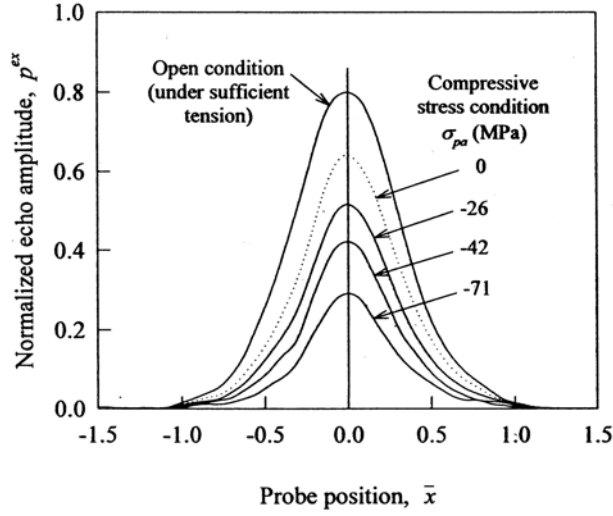


Figure 10 An example of normalized echo amplitude plotted as a function of normalized probe position.

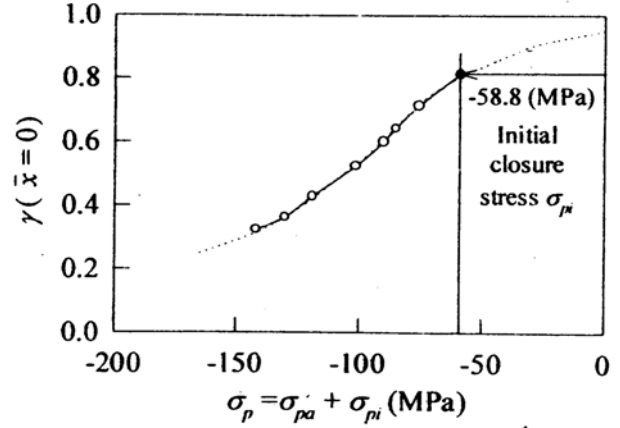


Figure 11 Reflection coefficient as a function of crack closure stress.

$$p_c^{es} = f_2(\bar{a}, \bar{x}). \quad (4)$$

Therefore, the desired estimated response  $p^{es}$  for closed crack in normalized form is expressed as

$$p^{es} = \mathcal{P} p_c^{es}. \quad (5)$$

Details of Eqs. (3) and (4) can be found in Ref. [21].

**Solution of Inverse Problem:** The essential feature of the ultrasonic evaluation method is to determine simultaneously the closure stress and the crack depth by comparing the estimated ( $p^{es}$ ) and the measured ( $p^{ex}$ ) amplitudes of the echo signals. For the best estimation, a suitable optimization algorithm is used to minimize an objective function,  $F$ , which is defined as follows:

$$F = \sum_{i=1}^n \left[ (p^{ex})_i - (p^{es})_i \right]^2, \quad (6)$$

where  $n$  is the total number of measurements corresponding to the discrete probe position.

**Evaluation Results and Discussions:** In order to verify the reliability of the present method, it was applied to a number of closed and open cracks, and the results are presented in Table 1. The evaluated results clearly verify that the crack closure stress as well as the crack size of smaller closed cracks can successfully be determined by using the present technique. The evaluated closure stress for any open crack is zero, which proves the validity of the technique. From the evaluated results of  $a$  and  $\sigma_p$ , the crack opening stress intensity factor  $K_{op}$  is determined from the following relation [22]:

$$K_{op} = |\sigma_p| \sqrt{\frac{2a}{\pi}} \int_0^1 (\xi^{-1/2} + m_1 \xi^{1/2} + m_2 \xi^{3/2}) d\xi, \quad (7)$$

where  $m_1 = 0.6147 + 17.1844\alpha^2 + 8.7822\alpha^6$ ,  $m_2 = 0.2502 + 3.2889\alpha^2 + 70.0444\alpha^6$ ,  $\alpha = a / T' \leq 0.5$ , and  $T'$  is the thickness of specimens having no notch. The evaluated values of  $K_{op}$  for closed cracks are presented in Table 1. In

determining  $K_{op}$  the crack contour is assumed two-dimensional for the sake of convenience, while the actual crack shape through the specimen width is three-dimensional because of the wide width of the specimens used. This assumption would be a good approximation for treating shallow crack where the three-dimensional effect is very little. The maximum and minimum values of stress intensity factor,  $K_{imax}$  and  $K_{imin}$ , averaged over the specimen width, used for preparation of crack are also presented in Table 1 for comparing them with the values of  $K_{op}$ . In Specimen B, the average value of  $K_{op}$  is near the value of  $K_{imin}$ . In Specimen C, on the other hand, the value of  $K_{op}$  ( $16.1 \text{ MPa}\cdot\text{m}^{1/2}$ ) is much bigger than that of  $K_{imin}$  ( $2.6 \text{ MPa}\cdot\text{m}^{1/2}$ ). The evaluation of  $K_{op}$  in fatigue crack bears significant importance for predicting the future crack growth, and we have succeeded it.

Table 1 Evaluated results and the actual crack depth

Specimen		$a$	$a$	$\sigma_p$	$K_{op}$	$K_{imax} / K_{imin}$
		actual (mm)	evaluated (mm)	evaluated (MPa)	estimated ( $\text{MPa}\cdot\text{m}^{1/2}$ )	used (av.) ( $\text{MPa}\cdot\text{m}^{1/2}$ )
Closed crack	B	0.82	0.95	-204	13.0	22.0 / 11.0
		1.45	1.33	-140	10.9	
		2.34	2.00	-88	9.0	
	C	3.45	3.20	-104	16.1	26.0 / 2.6
Open crack	B	0.82	0.80 <sup>1</sup>	0 <sup>1</sup>	—	—
		1.45	1.40 <sup>1</sup>	0 <sup>1</sup>	—	—
		2.34	2.35 <sup>1</sup>	0 <sup>1</sup>	—	—

<sup>1</sup> The values were evaluated from the data obtained under loading for opening the crack.

**Conclusions:** This paper described two advanced techniques for nondestructive ultrasonic evaluation of closed cracks. Firstly, we showed the technique utilizing the thermal stress induced by cooling a cracked part. It was shown by both of experiment and the finite element method that the thermal stress brought by the temperature decrease effectively opened a closed crack and enhanced the ultrasonic response of the crack. Also, we have nondestructively succeeded in quantitative evaluation of both the crack depth and the crack closure stress. The technique is based on the analysis of inverse problem, and capable of evaluating tightly closed cracks under a no load condition. From the evaluated crack depth and the crack closure stress, one can determine the crack opening stress intensity factor.

**Acknowledgements:** The authors are grateful to Mr. M. Mikami and Mr. T. Shōji of Tohoku University for their technical assistance in the experiments. This work was partly supported by the Ministry of Education, Culture, Sports, Science and Technology of Japan under Grant-in-Aid for Specially Promoted Research (COE)(2)11CE2003.

#### References:

- [1] R.J. Hudgell, L.L. Morgan and R.F. Lumb, Brit. J. NDT, Vol. 16, No. 5, pp. 144-149, 1974.
- [2] M.G. Silk, in *Research Techniques in Nondestructive Testing*, Vol. III, Academic Press, London, UK, 1977, pp. 51-99.
- [3] S. Golan, L. Adler, K.V. Cook, R.K. Nanstad and T.K. Bolland, J. Nondestr. Eval., Vol. 1, No. 1, pp. 11-19, 1980.
- [4] B.R. Tittmann and O. Buck, J. Nondestr. Eval., Vol. 1, No. 2, pp. 123-136, 1980.
- [5] O. Buck and B.R. Tittmann, in *Advances in Crack Length Measurement*, C.J. Beevers, ed., Engineering Materials Advisory Services, Warley, UK, 1982, pp. 413-446.
- [6] K. Date, H. Shimada and N. Ikenaga, NDT International, Vol. 15, No. 6, pp. 315-319, 1982.
- [7] O. Buck, R.B. Thompson and D.K. Rehbein, J. Nondestr. Eval., Vol. 4, No. 3/4, pp. 203-212, 1984.
- [8] K.K. So and A.N. Sinclair, Nondestructive Testing Communication, Vol. 3, No. 3, pp. 67-74, 1987.

- [9] F. Walte, W. Gebhardt and R. Hoffmann, in *Proc. 12th World Conference on Nondestructive Testing*, Vol. II, Elsevier, Amsterdam, The Netherlands, 1989, pp. 1695-1701.
- [10] D.A. Cook and Y.H. Berthelot, *NDT&E International*, Vol. 34, No. 7, pp. 483-492, 2001.
- [11] M. Saka, E. Schneider and P. Höller, *Res. Nondestr. Eval.*, Vol. 1, No. 2, pp. 65-75, 1989.
- [12] M. Saka and H. Abé, in *Computational and Experimental Fracture Mechanics*, Vol. 16, H. Nisitani ed., Computational Mechanics Publications, Southampton, UK, 1994, pp. 165-185.
- [13] R.L. Thomas, in *Review of Progress in QNDE*, Vol. 21, D.O. Thompson and D.E. Chimenti, eds., American Institute of Physics, New York, pp. 3-13, 2002.
- [14] M.A.S. Akanda, and M. Saka, *JSME Int. J., Series A*, Vol. 45, No. 2, pp. 252-261, 2002.
- [15] M. Saka and T. Uchikawa, *NDT&E International*, Vol. 28, No. 5, pp. 289-296, 1995.
- [16] S.R. Ahmed and M. Saka, *Trans. ASME, J. Pressure Vessel Technol.*, Vol. 120, No. 4, pp. 384-392, 1998.
- [17] S.R. Ahmed and M. Saka, *J. Nondestr. Eval.*, Vol. 21, No. 1, pp. 9-22, 2002.
- [18] M. Saka and M.A.S. Akanda, *Res. Adv. in Applied Physics*, Vol. 3, pp. 1-10, 2003.
- [19] M. Kikukawa, M. Jono, K. Tanaka and M. Takatani, *J. Soc. Materials Science, Japan*, Vol. 25, No. 276, pp. 899-903, 1976, in Japanese.
- [20] N.A. Fleck, in *Fatigue Crack Measurement: Techniques and Applications*, K.J. Marsh, R.A. Smith and R.O. Ritchie, eds., Engineering Materials Advisory Services, Warley, UK, 1991, pp. 69-93.
- [21] M. Saka and M.A.S. Akanda, *J. Nondestr. Eval.*, Vol. 23, 2004, in press.
- [22] H.F. Bueckner, in *Mechanics of Fracture*, G.C. Sih, ed., Noordhoff International Publishers, Leyden, The Netherlands, Vol. 1, 1973, pp. 239-314.